

## Predicting Controlled-Release Behavior of Degradable PLA-*b*-PEG-*b*-PLA Hydrogels

**Mariah N. Mason,<sup>†</sup> Andrew T. Metters,<sup>†</sup> Christopher N. Bowman,<sup>†,‡</sup> and Kristi S. Anseth<sup>\*,†,§</sup>**

*Department of Chemical Engineering and Howard Hughes Medical Institute, University of Colorado, Boulder, Colorado 80309-0424, Biomaterials Research Center, University of Colorado, Health Sciences Center, Denver, Colorado 80262*

*Received January 8, 2001; Revised Manuscript Received April 3, 2001*

**ABSTRACT:** This paper describes the development and application of scaling laws relating bulk-degradation behavior of poly(lactic acid)–poly(ethylene glycol)–poly(lactic acid) (PLA-*b*-PEG-*b*-PLA) copolymer hydrogels to the ever-changing transport properties during network degradation. Specifically, the relationships developed were used to extend previous work and to predict the effects of cross-linking density and hydrolytic degradation rate on the controlled release of high molecular weight proteins from these hydrogels. Theoretical drug release profiles, obtained using scaling laws, agree qualitatively with experimental observations and show a decrease in the protein release rate with an increase in protein size, extent of macromer functionalization, and macromer concentration. Quantitative predictions of release behavior were possible under certain experimental conditions.

### Introduction

Although hydrogels have enjoyed a long history of application as drug delivery vehicles (as well as contact lenses, super-absorbent materials, and adhesives), their usefulness is still limited. Equilibrium-swollen, non-degradable hydrogels are often restricted to drug release controlled by a near-constant diffusion coefficient that cannot yield the desired release profiles for particular applications. In addition, for advanced techniques such as drug delivery targeted to specific sites within the body, it is highly desirable to utilize a system that does not necessitate a second surgery for retrieval of the drug carrier. To address these issues, researchers have recently experimented with a novel class of degradable, polymeric hydrogels.

The successful application of hydrogels as controlled drug delivery vehicles is strongly linked to their excellent biocompatibility and flexibility in tailoring their physiochemical properties. Biodegradable hydrogels have emerged as a way to prepare new and improved drug delivery systems by synergistically combining the advantageous properties of traditional hydrogels with the flexibility of degradation mechanisms to control various aspects of the release behavior.<sup>1</sup> These degradable materials are particularly useful for the release of high molecular weight therapeutics, such as proteins and oligopeptides. While previous researchers have used degradable poly(ethylene glycol)-based hydrogels to release pharmaceuticals, few studies have been performed to correlate polymer degradation kinetics and subsequent changes in network structure with drug release.

To function effectively in any controlled-release application, the behavior of a degradable hydrogel must be predictable and well understood under a wide variety

of conditions. Previous work by Lu and Anseth<sup>2</sup> described a methodology for predicting drug release from degradable PLA-*b*-PEG-*b*-PLA hydrogels through knowledge of the time-dependent swelling behavior of their hydrophilic networks. A free-volume equation was used to relate the swelling dynamics of the degrading hydrogels to time-dependent diffusion coefficients for various solutes within the gels. This research qualitatively related release behavior of these degrading gels to the initial macromer architecture. The effect of PEG chain length, PLA block length, and solute size on the release behavior was documented. Drug release predictions based on a one-dimensional diffusion equation with a time-dependent diffusivity were shown to depend strongly on the relative rates of drug diffusion and network degradation and generally agreed with experimental results.

This paper aims to extend the usefulness of PLA-*b*-PEG-*b*-PLA hydrogels as controlled-release devices by relating their solute-release rates and profiles to their bulk-degradation behavior. A hybrid statistical and kinetic degradation model<sup>3,4</sup> was developed to predict the microscopic and macroscopic degradation behavior of these hydrogel systems. As a further extension to this model, a pseudo-first-order kinetic mechanism for the hydrolysis of network cross-links is incorporated through scaling laws to illustrate the direct impact of PLA hydrolysis kinetics on the network structure and transport properties. Once established, these relationships are used to predict the effects of chemical, structural, and degradation properties on the release of proteins from these gels. Experiments were performed to observe and quantify the release behavior and to verify the theoretical predictions.

### Experimental Section

The polymeric degradable hydrogel used in these studies was fabricated from a triblock PLA-*b*-PEG-*b*-PLA comonomer with acrylate end groups (see Figure 1). Each domain along this macromer plays a specific role in the resulting hydrogel function: the PEG backbone gives the hydrogel its hydrophilicity; the hydrolytically labile PLA linkages provide bio-

<sup>†</sup> Department of Chemical Engineering, University of Colorado.

<sup>‡</sup> Biomaterials Research Center, University of Colorado.

<sup>§</sup> Howard Hughes Medical Institute, University of Colorado.

\* To whom correspondence should be addressed. E-mail: Kristi.Anseth@Colorado.edu; Fax (303) 735-0095.

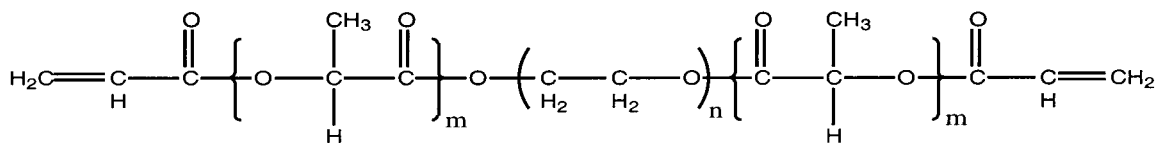


**Figure 1.** Chemical structure of the degradable PLA-*b*-PEG-*b*-PLA macromer.

**Table 1. Selected Characteristics of Degradable Macromers Determined Using  $^1\text{H}$  NMR<sup>a</sup>**

macromer	PEG MW (Da)	PLA block size ( <i>j</i> )	percent acrylation (= $Z \times 100\%$ )
1	3400	2.7	90
2	2000	2.2	70
3	2000	3.3	90
4	3400	6.2	80

<sup>a</sup> *j* is the average number of lactic acid repeat units per PLA block of the PLA-*b*-PEG-*b*-PLA macromer, and *Z* is the fractional extent of acrylate functionalization of the macromer chain ends.

**Table 2. Selected Properties of Released Solutes**

solute	MW (Da)	Stokes' radius (Å)	solubility in water at 25 °C (mg/mL)	estd diffusivity at 37 °C in aq soln ( $\times 10^{-4}$ mm <sup>2</sup> /s)
lysozyme	14 100	16.0	10.0	2.04
bovine serum albumin (BSA)	65 000	34.8	40.0	0.938

degradability; and the polymerizable end groups provide the means to form a cross-linked network. These macromers were synthesized according to the techniques first described by Sawhney et al.<sup>5</sup>  $^1\text{H}$  NMR spectroscopy (Varian VSR-500S) was used to characterize the structure of the block copolymers. The important characteristics of the macromers used in the current drug-release experiments are given in Table 1.

Photopolymerization of the macromers was initiated with a 365 nm light source (Blak-Ray; model B100 AP) having a peak intensity of approximately 15 mW/cm<sup>2</sup>. The solid macromer was dissolved in deionized water to a specified concentration, and a 20 wt% solution of the photoinitiator 2,2-dimethoxy-2-phenylacetophenone (Irgacure 651, Ciba Geigy) in ethanol was then added to the macromer solution until the initiator concentration was 0.02 wt%. For the release experiments, various solutes were also added to the macromer solution at concentrations up to 4.0 wt%. Photopolymerization of the final mixture produced hydrogel samples approximately 1.0 cm in diameter and 1.0 mm thick.

Two hydrophilic macromolecular proteins were used in the controlled-release studies: bovine serum albumin (BSA) and lysozyme (Sigma). Listed in Table 2 are the molecular weights of the solutes along with their Stokes' radius and solubility in water at 25 °C.<sup>6</sup> An estimation of the solute diffusivity in dilute aqueous solution at 37 °C was calculated using the Stokes–Einstein equation (eq 1), and the results are also presented in Table 2.

$$D_0 = \frac{k_B T}{6\pi\eta r_s} \quad (1)$$

In this equation,  $r_s$  is the Stokes–Einstein hydrodynamic radius of the solute;  $k_B$  is Boltzmann's constant;  $T$  is the temperature;  $\eta$  is the viscosity of the solution; and  $D_0$  is the solute diffusivity.

Degradation and solute release were conducted in a 7.4 pH phosphate buffered solution (PBS, Fisher) at 37 °C. Each gel was separately placed in a vial containing a large excess (10 mL) of the PBS buffer to maintain sink conditions. At specified time points, swelling and drug release measurements were made. To obtain the volumetric swelling ratio of the gels ( $Q$ ), a disk was removed and weighed in air ( $W_{A,S}$ ) and in heptane ( $W_{H,S}$ ). The polymer weight ( $W_{A,D}$ ) was obtained by drying the

sample under vacuum until constant weight.  $Q$  was then calculated as described previously.<sup>3</sup>

For solute release experiments, 0.5 mL samples of the vial buffer solution were taken and replaced by fresh buffer. After accounting for dilution caused by previous measurements, protein concentrations were measured with a Bio-Rad protein assay using the microassay procedure, in which a differential color change of the dye occurs in response to various concentrations of protein.<sup>7</sup> The color change was subsequently monitored by measuring the absorbance at 596 nm on a UV–Vis spectrophotometer (Hewlett-Packard 8452A diode array).

## Results and Discussion

**Characterization of Network Transport.** From the experimentally measured volumetric swelling ratio of a hydrogel ( $Q$ ), one can calculate directly the average molecular weight between cross-links ( $\bar{M}_c$ ) and the polymer volume fraction ( $v_2$ ) of a given network.<sup>8</sup> From this information, various network parameters that are important for controlled release applications can be calculated. For example, the mesh size of a hydrogel network ( $\xi$ ) can be determined as described by Canal and Peppas:<sup>9</sup>

$$\xi = v_2^{-1/3} (\bar{r}_0^2)^{1/2} \quad (2)$$

where  $(\bar{r}_0^2)^{1/2}$  is the root-mean-squared end-to-end distance of the polymer chains in the unperturbed state.

For homogeneous hydrogels, numerous equations exist to describe the relationship between diffusivity and network structure. A free-volume approach developed by Lustig and Peppas<sup>10</sup> was chosen for this research because of its proven accuracy and application for PEG-based hydrogels:

$$\frac{D_g}{D_0} = \left(1 - \frac{r_s}{\xi}\right) \exp\left(-Y \left(\frac{v_2}{1 - v_2}\right)\right) \quad (3)$$

In this relationship,  $D_g$  is the solute diffusivity in a swollen gel;  $D_0$  is the solute diffusivity in the swelling solvent;  $r_s$  is the radius of the solute; and  $Y$  is the ratio of the critical volume required for a successful translational movement of the solute molecule to the average free volume per molecule of the liquid.

**Scaling Laws for Drug Release.** The network mesh size and solute diffusivity in highly swollen PLA-*b*-PEG-*b*-PLA hydrogels are related through the average molecular weight between cross-links ( $\bar{M}_c$ ). A simplified form of the Flory–Rehner equation indicates that the volumetric swelling ratio ( $Q$ ) is proportional to the cross-linking density of a hydrogel ( $\rho_c$ ) raised to the  $-3/5$  power when the gel is highly swollen ( $v_2 < 0.1$ ). Since  $\rho_c$  and  $\bar{M}_c$  are inversely proportional, this equation implies that  $Q$  and  $\bar{M}_c$  scale in a similar manner as given by:

$$Q \sim (\bar{M}_c)^{3/5} \quad (4)$$

Combining eqs 2 and 4 and recognizing that  $\bar{r}_0^2$  is

proportional to  $\overline{M}_c$ , a scaling relationship between the network mesh size and the average molecular weight between cross-links is given by:

$$\xi = Q^{1/3}(\overline{r}_0^2)^{1/2} \sim (\overline{M}_c)^{7/10} \quad (5)$$

For high degrees of swelling ( $v_2 < 0.1$ ), the exponential term of eq 3 can be neglected to yield the following simplified equation for solute diffusivity:

$$\frac{D_g}{D_0} = 1 - \frac{r_s}{\xi} \quad (6)$$

Combining eqs 5 and 6 produces the final scaling relationship between  $\overline{M}_c$  and the solute diffusion in these highly swollen gels:

$$1 - \frac{D_g}{D_0} = \frac{r_s}{\xi} \sim (\overline{M}_c)^{-7/10} \quad (7)$$

**Correlation of Drug Release to Degradation Kinetics.** The physical network parameters and solute diffusion coefficient were related directly to the kinetics of PLA hydrolysis and degradation time through an understanding of degradation behavior of cross-linked hydrogels and its impact on network microstructure. Experimentally observed exponential changes in the macroscopic properties of PLA-*b*-PEG-*b*-PLA hydrogels with degradation (e.g., swelling and compressive modulus) can be explained by the justifiable assumption of a pseudo-first-order kinetic equation for the hydrolysis of network cross-links.<sup>3</sup> The first-order hydrolysis kinetics equation is given by:

$$\frac{dn_E}{dt} = -k_E' n_E \quad (8)$$

where  $n_E$  represents the number of moles of ester bonds and  $k_E'$  is the pseudo-first-order reaction rate constant for the hydrolysis of a single lactide ester linkage.

To reduce the kinetic equation for hydrogel degradation to the simplified form of eq 8, the acid concentration as well as the water concentration during degradation is assumed constant. All experiments were performed in a phosphate buffered solution, which kept the solution at a constant pH of 7.4 throughout the entire degradation process. Since the hydrogels used in this study were copolymers with the PLA blocks contributing only a small fraction to the overall molecular weight, the total acid group concentration in the gels is relatively low. In addition, the highly swollen nature of the gels, due to the presence of the hydrophilic PEG blocks, lowers the concentration of acid species within the cross-linked networks even further while allowing for efficient removal of acidic degradation products. Finally, because of the highly swollen nature of these gels, the water concentration remains relatively constant throughout degradation.

Therefore, as the ester groups and cross-links within these hydrogels are hydrolyzed and degradation proceeds, pseudo-first-order kinetics dictate an exponential increase in the average molecular weight between cross-links.<sup>3</sup> The exponential change in the molecular weight between cross-links is related to the physical and kinetic

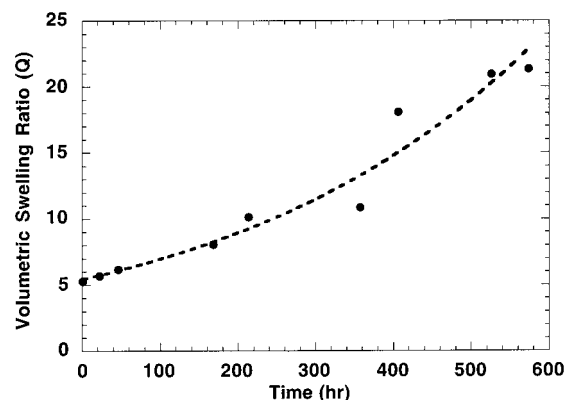


**Figure 2.** Experimentally measured volumetric swelling ratio vs degradation time for a typical PLA-*b*-PEG-*b*-PLA hydrogel. The dashed line represents the exponential model fit to the data with a pseudo-first-order hydrolysis rate constant,  $k_E'$ , of  $1.0 \times 10^{-5} \text{ min}^{-1}$ .

characteristics of the degrading hydrogel as given by:

$$\overline{M}_c \sim e^{2jk_E't} \quad (9)$$

where  $j$  represents the number of ester bonds per PLA block in a PLA-*b*-PEG-*b*-PLA cross-link and  $t$  is the degradation time.<sup>4</sup> The factor of two in the exponential rate constant of eq 9 occurs because there are two PLA blocks per cross-link (Figure 1). In the PLA-*b*-PEG-*b*-PLA network, the degradation of one or more ester bonds leads to the cleavage of a cross-link.

Equations 4 and 9 can be combined to give the following expression for the swelling ratio as a function of degradation time for the PLA-*b*-PEG-*b*-PLA hydrogels:

$$Q \sim e^{(6/5)jk_E't} \quad (10)$$

Due to the exponential character of the pseudo-first-order hydrolysis kinetics with time, the scaling proportionality between  $Q$  and  $\overline{M}_c$  given in eq 4 is incorporated directly into the exponent on the right-hand side of eq 10. The mesh size and solute diffusion coefficient within these gels, as functions of degradation time, can also be scaled:

$$\xi \sim e^{(7/5)jk_E't} \quad (11)$$

$$1 - \frac{D_g}{D_0} = \frac{r_s}{\xi} \sim e^{(-7/5)jk_E't} \quad (12)$$

Equations 10 through 12, therefore, predict an exponential dependence for the volumetric swelling ratio, network mesh size, and solute diffusivity in PLA-*b*-PEG-*b*-PLA gels as a function of degradation time. Figure 2 shows one of many experimental measurements performed to verify the exponential behavior of the swelling ratio as a function of degradation time in these gels.

In eqs 10 through 12, the PLA block size ( $j$ ) is controlled during macromer synthesis and experimentally measured by  $^1\text{H}$  NMR (Table 1). From the swelling data, therefore, a value for  $k_E'$  is readily calculated. Using this value for  $k_E'$  in eqs 11 and 12,  $\xi$  and  $(1 - D_g/D_0)$  are predicted readily throughout the course of hydrogel degradation. As shown in Figure 3, the average mesh size within the hydrogel increases exponentially



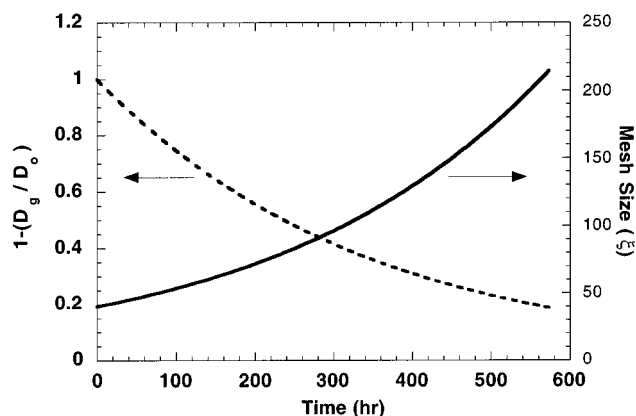


**Figure 3.** Mesh size of the degrading hydrogel and the normalized solute diffusivity as functions of degradation time.

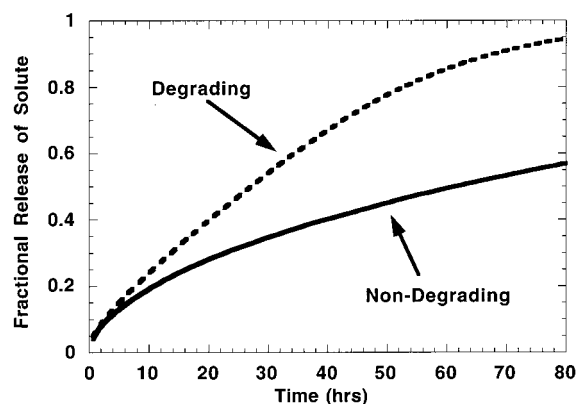
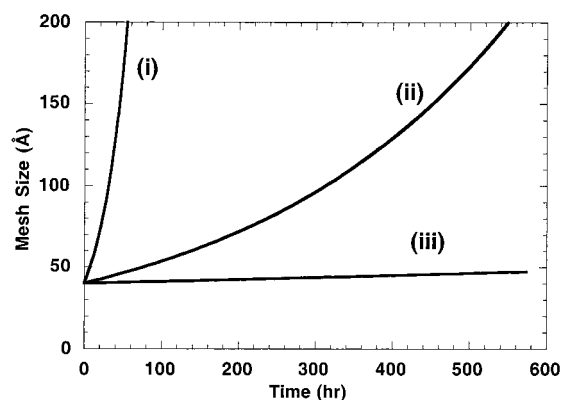


**Figure 4.** Predicted fractional release of BSA as a function of time from a nondegrading hydrogel (solid line) and a degrading gel (dashed line) shown in Figure 3. Both gels have an initial mesh size of 41 Å.

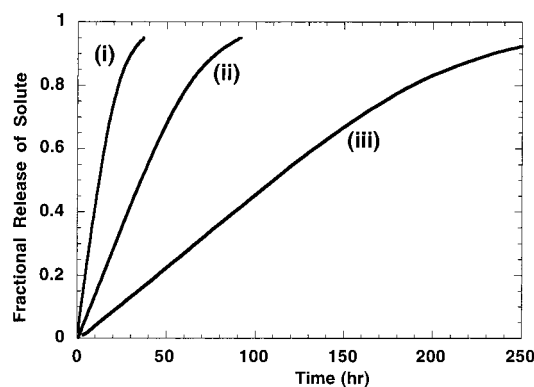
with the systematic degradation of network cross-links. This increase in mesh size leads to an increase in mobility for an encapsulated solute as quantified through its increasing diffusion coefficient ( $D_g$ ). However, the diffusion coefficient for the trapped solute only increases to a limiting value,  $D_0$ .

Solute release from nondegradable hydrogels is known to be a function of a variety of chemical and physical parameters that influence the mesh size of the network. As shown by West and Hubbell<sup>1</sup> and Lu and Anseth,<sup>2</sup> the release behavior of PLA-*b*-PEG-*b*-PLA hydrogels is also influenced by their degradation behavior. Equations 11 and 12 allow the influence of hydrogel degradation on solute release to be readily quantified and predicted.

The time-dependent function for the solute diffusion coefficient, eq 12, was used to predict solute release from a degrading PLA-*b*-PEG-*b*-PLA hydrogel disk using the one-dimensional diffusional release equation for a uniformly loaded film.<sup>11</sup> Using the calculated degradation behavior from Figure 3, fractional release profile of BSA from the same PLA-*b*-PEG-*b*-PLA hydrogel was predicted and is shown in Figure 4. The predicted release profile of an initially similar, yet nondegrading, gel is also plotted for comparison. This figure illustrates how the hydrolysis of cross-links within the network increases the mesh size and solute diffusion coefficient and enhances the BSA release rate. The overall release profile of the degrading system also has a different shape than that of an equilibrium-swollen, nondegrading system.



(A)



(B)

**Figure 5.** (A) Network mesh size and (B) predicted fractional release of BSA as a function of degradation time for gels with varying degradation rates: (i)  $K' = 3.3 \times 10^{-4} \text{ min}^{-1}$ ; (ii)  $K' = 3.3 \times 10^{-5} \text{ min}^{-1}$ ; (iii)  $K' = 3.3 \times 10^{-6} \text{ min}^{-1}$ .

A number of parameters affect the initial structure of a hydrogel, its degradation rate, or both. Most often, these changes are reflected in an increasing or decreasing value for  $K'_E$  or  $K'$  ( $= jK'_E$ ). For example, increasing the number of ester bonds per PLA block ( $j$ ) increases the gel degradation rate.<sup>4</sup> Also, increasing the extent of functionalization or the macromer concentration during network formation leads to lower degradation rates through decreased values of  $K'_E$ .<sup>4</sup> Using eqs 11 and 12, Figure 5a shows the effect of increasing the overall degradation rate constant,  $K'$ , on the mesh size of the gel as a function of degradation time. Differences in the mesh size and other characteristics of these networks dramatically affect the solute-release profiles predicted from these gels, as shown in Figure 5b.

**Comparison of Experimental and Predicted Release Profiles.** A number of experimental drug-release studies were performed to assess the suitability of the scaling laws to correlate drug-release to network degradation kinetics. In the first study, two macromolecular solutes of different molecular weights were released from the same degrading network. The volumetric swelling curves, and therefore degradation rates of the two systems, are identical. From eqs 3 and 7, the diffusion coefficients of both systems scale identically with degradation time, but the absolute values of the diffusion coefficients depend on the solute size ( $r_s$ ). As  $r_s$  increases,  $D_g/D_0$  decreases, and thus, smaller solute molecules are released more rapidly. As shown by the release profiles in Figure 6, this trend is observed for lysozyme ( $r_s = 16 \text{ Å}$ ) and BSA ( $r_s = 35 \text{ Å}$ ) with the smaller lysozyme protein being released more quickly.

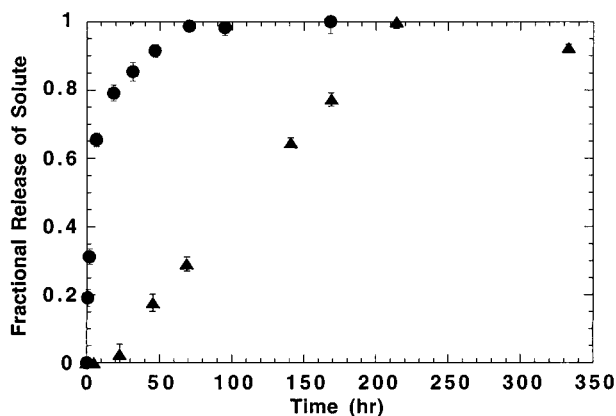
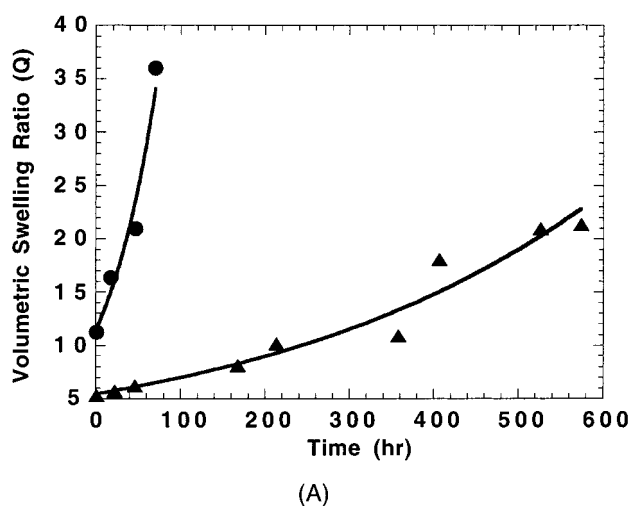
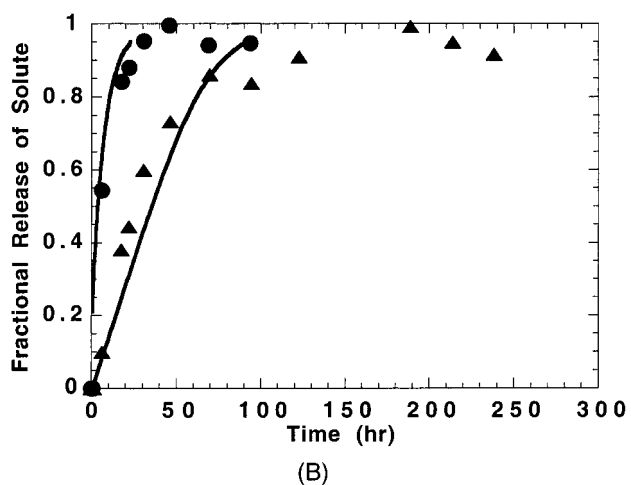


**Figure 6.** Experimentally measured release of (●) lysozyme and (▲) BSA from a hydrogel formed from a 30 wt% solution of macromer 1 from Table 1. Error bars represent one standard deviation.



(A)



(B)

**Figure 7.** (A) Volumetric swelling ratio and (B) fractional release of BSA as a function of degradation time from two PLA-*b*-PEG-*b*-PLA hydrogels with varying extents of acrylate functionalization: (●)  $Z = 70 \pm 5\%$  and (▲)  $Z = 90 \pm 5\%$ . Lines represent exponential fits to the swelling data (A) and solute release predictions based on scaling equations (B).  $D_0 = 1.0 \times 10^{-5} \text{ mm}^2/\text{s}$  for both curves.

Release experiments were also measured from two hydrogels with different extents of acrylate functionalization,  $Z$ . As  $Z$  decreases, the initial cross-linking density decreases (increasing the initial swelling ratio and mesh size), as shown in Figure 7a, and the

degradation rate dramatically increases. Both of these effects cause an increase in the drug release rate as seen in Figure 7b.

Predictions for the release behavior based on initial characteristics of the gels and their degradation rates are shown by the lines in Figure 7b. In this case, theoretical predictions match experimental release profiles very well. The agreement between theoretical and experimental results demonstrates that the scaling equations developed in this work are useful in relating the degradation properties of a hydrogel to its solute release behavior.

To determine the impact that the initial macromer concentration has on the release behavior of PLA-*b*-PEG-*b*-PLA hydrogels, solute release was measured from a series of hydrogels formed from increasing concentrations of the same macromer. Increasing the solvent concentration during polymerization of these hydrogels has many direct influences on their network structure including increased cyclization.<sup>12</sup> From the theoretical kinetic equations for initiation, propagation, and termination, one quickly realizes that the kinetic chain lengths will be lowered to some extent with an increase in solvent concentration. In addition, the initiation efficiency and the degree of autoacceleration during polymerization will also decrease. Although the effect of each of these changes may be small, lumped together they act to form dramatically different network structures with different degradation and solute release behaviors.<sup>3</sup>

The swelling behaviors of gels formed from different macromer concentrations are shown in Figure 8a. As the macromer concentration in the polymerized solution is increased from 25 to 50 wt%, the degradation rate, as measured from the exponential swelling curves, doubles even though the initial swelling ratios increase only slightly. The experimentally measured solute release behavior from these three systems is shown in Figure 8b. These data, along with those presented in Figure 7, demonstrate the effect of hydrogel degradation rate on solute release behavior in the PLA-*b*-PEG-*b*-PLA systems. As the degradation rate increases, the solute is released at a faster rate, and the shape of the release profile vs degradation time changes. Theoretical predictions for this behavior are given by the series of solid lines. The time-dependent solute diffusion coefficient for these predicted profiles was described and correlated to the degradation kinetics of each respective system using eq 12. Although the qualitative trends of the three data sets are matched by the model predictions, reasonable fits to the release of all three hydrogels cannot be obtained when the same limiting diffusion coefficient ( $D_0$ ) is used for all systems. Quantitative model fits to all data sets can only be obtained if  $D_0$  is allowed to decrease with macromer concentration. These results indicate fundamental differences in the network structure that cannot be entirely explained by the current physical description of the initial network and its subsequent degradation.

## Conclusions

Scaling laws were developed to understand the solute-release behavior of PLA-*b*-PEG-*b*-PLA hydrogels. The structural and transport characteristics of these degrading hydrogels, which impact their application as controlled release devices, were related to the network cross-linking density and their hydrolytic degradation

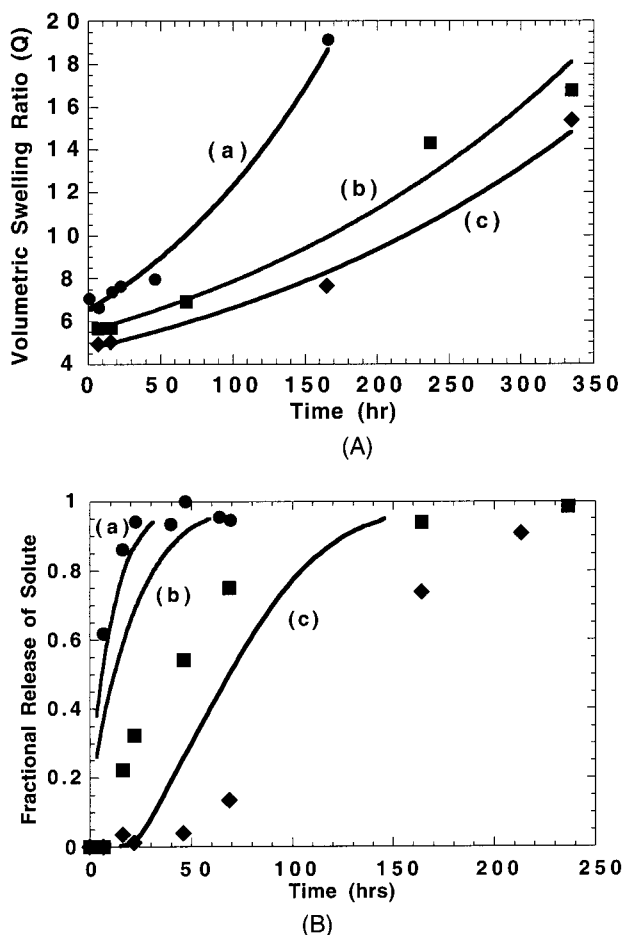


**Figure 8.** (A) Volumetric swelling ratio and (B) fractional release of BSA as a function of degradation time from a series of PLA-*b*-PEG-*b*-PLA hydrogels polymerized from increasing concentrations of macromer: (●) 25 wt%, (■) 35 wt%, and (◆) 50 wt%. Lines represent exponential fits to the swelling data (A) and solute release predictions based on scaling equations (B).  $D_0 = 1.0 \times 10^{-5} \text{ mm}^2/\text{s}$  for all curves.

rate. The effects of degradation rate on the network mesh size, solute diffusivity, and drug release profile

were predicted. These relationships were used to model and predict drug release profiles from degradable PLA-*b*-PEG-*b*-PLA gels. The predicted drug-release profiles agree qualitatively with experimental observations, which show a decrease in the solute release rate with an increase in solute size, extent of acrylate functionalization, and macromer concentration. Though qualitative behavior is accurately predicted, quantitative predictions of the variations in solute release behavior with initial macromer concentration could not be made. This limitation is primarily attributed to either a deficiency in the solute diffusivity equation applied to the networks or a fundamental difference in the initial network structures.

**Acknowledgment.** The authors thank the National Science Foundation and the Rubber Division of the American Chemical Society for support of this work through fellowships to A.T.M. as well as a grant from the National Institutes of Health (DE12998). Additional support was made possible by a Beverly Sears Graduate Student Grant Award from the Graduate School and a grant from the Undergraduate Research Opportunities Program of the University of Colorado at Boulder.

## References and Notes

- (1) West, J. L.; Hubbell, J. A. *React. Polym.* **1995**, *25*, 139.
- (2) Lu, S.; Anseth, K. *Macromolecules* **2000**, *33*, 2509.
- (3) Metters, A.; Bowman, C.; Anseth, K. *Polymer* **2000**, *41*, 3993.
- (4) Metters, A.; Bowman, C.; Anseth, K. *J. Phys. Chem. B* **2000**, *104*, 7043.
- (5) Sawhney, A.; Chandrashekhara, P.; Hubbell, J. *Macromolecules* **1993**, *26*, 581.
- (6) Amsden, B. *Macromolecules* **1998**, *31*, 8382.
- (7) Bradford, M. M. *Anal. Biochem.* **1976**, *72*, 248.
- (8) Flory, P. *Principles in Polymer Chemistry*; Cornell University Press: Ithaca, NY, 1953.
- (9) Canal, T.; Peppas, N. A. *J. Biomed. Mater. Res.* **1989**, *23*, 1183.
- (10) Lustig, S. R.; Peppas, N. A. *J. Appl. Polym. Sci.* **1988**, *36*, 735.
- (11) Crank, J. *The Mathematics of Diffusion*; Clarendon Press: Oxford, 1975.
- (12) Elliott, J.; Anseth, J.; Bowman, C. *Chem. Eng. Sci.*, in press.

MA010025Y